

Cite this: *RSC Adv.*, 2019, 9, 20356

Regioselective microwave synthesis and derivatization of 1,5-diaryl-3-amino-1,2,4-triazoles and a study of their cholinesterase inhibition properties†

Sabrina Neves Santos,^{ab} Gabriela Alves de Souza,^{ab} Thiago Moreira Pereira,^{ab} Daiana Portella Franco,^{ab} Catarina de Nigris Del Cistia,^b Carlos Mauricio R. Sant'Anna,^b Renata Barbosa Lacerda^{ab} and Arthur Eugen Kümmerle^{ab} ^{*ab}

Herein we describe the development of an efficient one-pot regioselective synthesis protocol to obtain *N*-protected or *N*-deprotected 1,5-diaryl-3-amino-1,2,4-triazoles from *N*-acyl-*N*-Boc-carbamidothioates. This improved protocol using microwave irradiation and low reaction times (up to 1 h) furnished desired compounds in yields ranging from 50 to 84%. This chemistry is useful for a variety of aromatic groups with electronically diverse substituents. The design and correct derivation of the amino group led to compounds able to inhibit cholinesterases with good IC₅₀ of up to 1 μM. Also, the mode of action (mixed-type) and SAR analysis for this series of compounds was described by means of kinetic and molecular modelling evaluations, showing potential for this class of compounds as new scaffolds for this biological activity.

Received 30th May 2019
Accepted 22nd June 2019

DOI: 10.1039/c9ra04105b

rsc.li/rsc-advances

Introduction

The five-membered azaheterocycle aminotriazole is widely described in the literature and has received great attention from the scientific community due to its diversity of biological activities. This increased attention to this 1,2,4-triazole nucleus comes from its possible non-classical bioisosteric replacement of a *cis*-amide bond from bioactive compounds.¹ 3-amino-1,2,4-triazoles have been described as an anti-inflammatory agent (A),² as a treatment for bronchial asthma (B),³ as an inhibitor of methionine aminopeptidase (C)⁴ and a NPY receptor,⁵ and as a selective positive allosteric modulator of the α7 nicotinic acetylcholine receptor (D)^x (Fig. 1).⁶

Several procedures have already been described for the synthesis of general 3-amino-1*H*-1,2,4-triazoles, with great attention to solid phase, microwaves and combinatorial synthesis.⁷ However, few of them explored the synthesis of 1,5-diaryl-3-amino-1,2,4-triazoles. The first methodology, described by Katritzky⁸ and also adapted to solid phase synthesis by Houghten,⁹ employs a cyclization reaction from an electrophilic

moiety (*N*-acylguanidines derived from benzotriazole or *N*-acyl carbamidothioate) and a nucleophilic one (alkyl or substituted aryl hydrazines) (Fig. 2). Unfortunately, these processes suffer from long reaction times, few examples, and low yields when both substitutions are aryl groups. Furthermore, in many cases they were unable to produce 3-*N,N*-unsubstituted amino triazole compounds.

The second methodology, described by Szilagyi,² is based on a two steps mechanism: the opening of 1,3,4-oxadiazolium perchlorate nucleus by the nucleophile cyanamide followed by its recyclization (Fig. 2). Despite better in scope and reactional yields compared to the Katritzky method, the explosive nature of perchloric acid and perchlorate salts

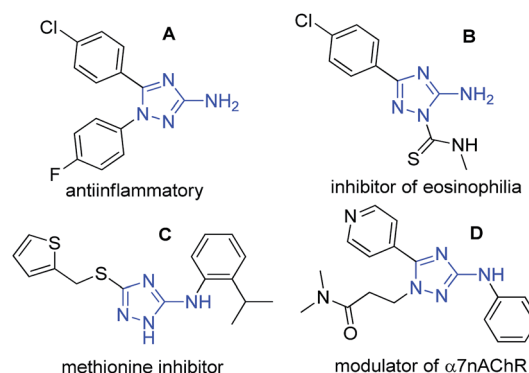


Fig. 1 Bioactive compounds with 3-amino-1,2,4-triazole nucleus.

^aLaboratório de Diversidade Molecular e Química Medicinal (LaDMol-QM, Molecular Diversity and Medicinal Chemistry Laboratory), Chemistry Institute, Universidade Federal Rural do Rio de Janeiro, Seropédica, Rio de Janeiro, 239897-000, Brazil. E-mail: akummerle@hotmail.com

^bPrograma de Pós-Graduação em Química (PPGQ), Universidade Federal Rural do Rio de Janeiro, Seropédica, Rio de Janeiro, 239897-000, Brazil

† Electronic supplementary information (ESI) available. See DOI: 10.1039/c9ra04105b



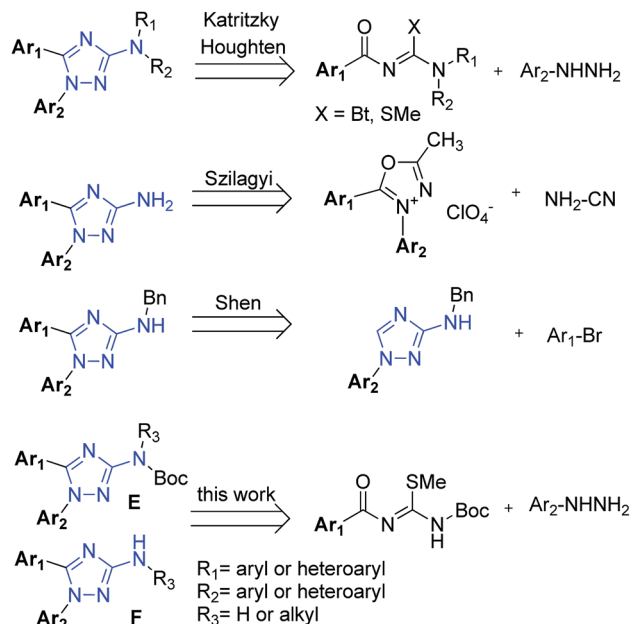


Fig. 2 Described synthetic strategies for the synthesis of 1,5-disubstituted 3-amino-1H-1,2,4-triazoles and our strategy for this work.

makes this methodology dangerous and not indicated to scale-up synthesis.^{10,11}

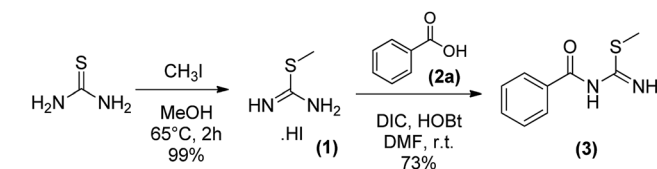
The third procedure was recently described by Shen,¹² presenting an interesting strategy for the C-arylation of amino-triazoles at position 1 by means of a Negishi coupling (Fig. 2). Despite of good yields and scope demonstrated, the high cost of this reaction associated with its drastic conditions in the final deprotection (6 M H₂SO₄, 80 °C, 16 h) can make this reaction limited in some cases. Thus, new simpler and more effective methodologies for the synthesis of 1,5-diaryl-3-amino-1,2,4-triazoles are still required.

Our goals in this work were: (1) to develop a simple one-pot regioselective synthesis protocol to obtain *N*-protected (E) or *N*-deprotected (F) 1,5-diaryl-3-amino-1,2,4-triazoles (Fig. 2) in low reaction times and suitable for diverse R₁ and R₂ aromatic groups, through an improvement of Katritzky procedure using *N*-acyl-*N*-Boc-carbamidothioates; (2) given the importance of microwave irradiation to heterocyclic chemistry,¹³ we decided to evaluate its influence in our synthesis. Furthermore, this technique proved to be suitable to furnish different 1,2,3 and 1,2,4 triazole derivatives in good yields and low reaction times;^{7b} (3) derivatization studies of *N*-protected compounds E to furnish series F, when R₃ is an alkyl group; and (4) use of *N*-derivatizations to correct design and obtain new 1,5-diaryl-3-amino-1,2,4-triazole derivatives as inhibitors of cholinesterases.

Results and discussion

Synthesis of triazoles

Our initial objective was to obtain the 1,5-diaryl-3-amino-1,2,4-triazoles (6) without any protection. For this purpose, we



Scheme 1 Synthesis of methyl *N*-acylthiourea (3).

planned a three-steps protocol (Schemes 1 and 2). The first step was the synthesis of *S*-methylisothiourea (1) as previously described,¹⁴ by the alkylation of urea with methyl iodide followed by precipitation and filtration (99% yield). The second step was the synthesis of *S*-methyl-*N*-benzoyl-isothiourea (3) in 73% yield from the reaction of *S*-methylisothiourea with an activated benzotriazole intermediate, previously obtained from the *in situ* reaction of benzoic acid (2a) with *N,N'*-diisopropylcarbodiimide (DIC) and 1-hydroxybenzo-triazole (HOBT) (Scheme 1).

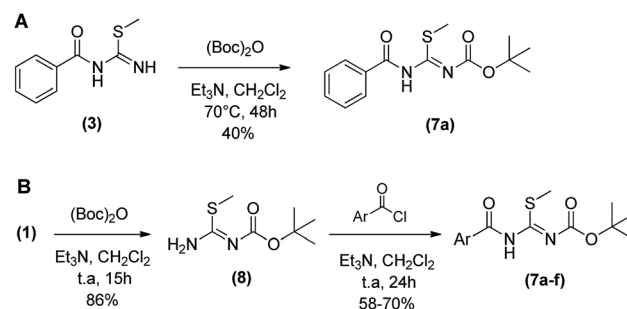
The cyclization reaction leading to 1,5-diphenyl-3-amino-1,2,4-triazole (6a) was performed in the last step by reacting *N*-benzoylthiourea (3) with phenylhydrazine (4). This reaction was attempted in two different solvents and heating sources (Table 1). The best reactional yield was observed for the conventional heating at 100 °C in acetonitrile.

However, long reaction time (48 h) was required to observe the consumption of reactants (Table 1, entry 3) and, although 75% of 6a could be obtained, 13% of its regioisomer (5) was also formed, complicating their chromatographic separation.

Bearing in mind the possible low reactivity and the lack of selectivity demonstrated by 3, we decided to introduce an electron withdrawing group at $-\text{C}=\text{NH}(\text{S}-\text{CH}_3)$ moiety by means of a labile *tert*-butyloxycarbonyl group ($-\text{Boc}$).

The synthesis of *N*-protected *N*-acyl-*S*-methylisothiourea (7) was evaluated reacting 3 with di-*tert*-butyl dicarbonate in dichloromethane at 70 °C in a sealed borosilicate tube. However only 40% of product 7 was furnished after 48 h (Scheme 2A). Aiming at to optimize the reaction process to obtain 7, a new synthetic route was evaluated (Scheme 2B).

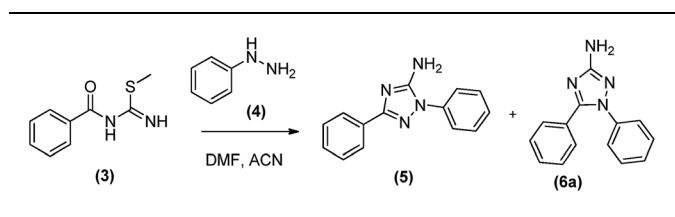
Instead of protecting the low reactivity *N*-acyl-*S*-methylisothiourea (3) in the least step, the new process started with the protection of *S*-methylisothiourea (1) in a similar condition as above described, furnishing the *N*-Boc-*S*-methylisothiourea (8)



Scheme 2 Synthesis of *N*-Boc-*S*-methylisothiourea derivatives (7).



Table 1 Synthesis of 1,5-diphenyl-3-amino-1,2,4 triazole (6a)



Entry	Solv.	Temp.	Time	(5) ^c %	(6a) ^c %
1	DMF	100 ^a	48 h	—	46
2	DMF	100 ^b	2 h	—	41
3	ACN	100 ^a	4 h	13	75
4	ACN	100 ^b	2 h	Trace	35

^a Conventional heating. ^b Microwave heating. ^c Isolated yields.

as a white solid in 86% yield after 15 h. Subsequently, **8** was reacted with correspondent acid chlorides in dichloromethane at room temperature for 24 hours, leading to the desired intermediates (**7a–f**) in yields ranging from 58 to 80%. This new synthetic route was more suitable for obtaining the *N*-acyl-*S*-methylisothiourea derivatives (**7a–f**) with higher yields and lower reaction times. In order to evaluate the reactivity and selectivity of the *N*-protected *N*-acyl-*S*-methylisothiourea (**7a**), we started the cyclocondensations maintaining the same temperature and solvents described before (*i.e.* DMF or acetonitrile as solvent and 100 °C) and the Table 2 shows the main results obtained.

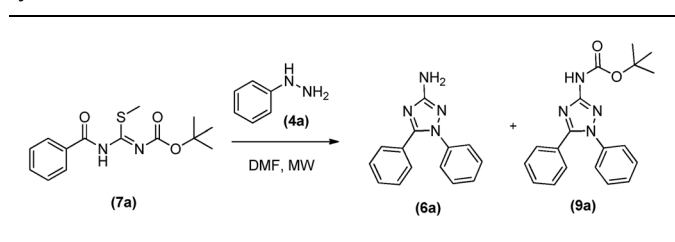
Initially the reactions were done without microwave assistance (Table 2, entries 1–4). Depending on the reaction time it was possible to observe that the cyclocondensation has occurred and the 1,5-diphenyl-3-amino-1,2,4-triazole could be

isolated in its both protected (with BOC group) (**9a**), after reaction of up to 40 min (Table 2, entries 1 and 3), and deprotected form (**6a**), in the case when DMF was used as solvent in 48 h of reaction (Table 2, entry 2). Curiously, longer reaction times in acetonitrile led to a by-product that we were not able to identify, without any trace of targeted 1,5-diphenyl-3-amino-1,2,4-triazoles (**6a** and **9a**) by the end of reaction (Table 2, entry 4).

In fact, as previous related for others amino-triazoles,^{7b} the use of microwave irradiation proved to be efficacious in increasing reactional yields, leading to the protected product **9a** in yields of up to 90% in 40 minutes (Table 2, entry 7), as well as being very efficient in obtaining the final deprotected 1,5-diphenyl-3-amino-1,2,4-triazole (**6a**), in shorter reaction time (1 h) and higher yield (82%) (Table 2, entry 6) compared to conventional heating. Once more, the reaction in acetonitrile at 150 °C led to the formation of the unknown by-product as previous described for the conventional heating (Table 2, entry 8). Therefore, DMF was chosen as the best solvent to synthesise the desired products, allowing the selective formation of the protected and deprotected 1,5-diphenyl-3-amino-1,2,4-triazoles, depending only on the temperature and reaction time.

With this set of conditions, the scope of reaction was evaluated varying the aromatic rings coming from both benzoic acid and phenylhydrazine reactants (Table 3). The cyclocondensations furnished the functionalized 1,5-diaryl-3-amino-1,2,4-triazoles in their protected and deprotected forms (**9a–h** and **6a–f**) in reasonable to good yields ranging from 47 to 90% in reactions of up to 1 hour. For all compounds, the

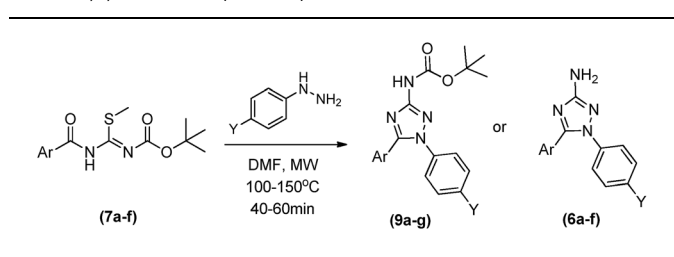
Table 2 Optimization of 1,5-diphenyl-3-amino-1,2,4 triazole (6a) synthesis



Entry	Solv.	Temp.	Time	6a % ^c	9a % ^c
1	DMF	100 ^a	40 min	—	71
2	DMF	100 ^a	48 h	76	—
3	ACN	100 ^a	40 min	—	74
4	ACN	100 ^a	48 h	—	—
5	DMF	100 ^b	40 min	—	79
6	DMF	150 ^b	60 min	82	—
7	ACN	100 ^b	40 min	—	87
8	ACN	150 ^b	60 min	—	—

^a Conventional heating. ^b Microwave heating. ^c Isolated yields.

Table 3 Scope of microwave-assisted synthesis of 1,5-diphenyl-3-amino-1,2,4-triazoles (6 and 9)



Prod.	Ar	Y	Time ^a	Temp. ^b	Yield ^c
9a	Ph	H	40	100	87
9b	4-OCH ₃ -Ph	H	40	100	62
9c	4-Cl-Ph	H	40	100	71
9d	4-NO ₂ -Ph	H	40	100	80
9e	Ph	NO ₂	40	100	61
9f	Ph	SO ₂ CH ₃	40	100	84
9g	4,5-DiBr-2-pyrrol	H	40	100	90
9h	2-Pyrrol	H	40	100	79
6a	Ph	H	60	150	82
6b	4-OCH ₃ -Ph	H	60	150	47
6c	4-Cl-Ph	H	60	150	68
6d	4-NO ₂ -Ph	H	60	150	52
6e	Ph	NO ₂	60	150	73
6f	Ph	SO ₂ CH ₃	60	150	69

^a Time in minutes. ^b Temperature in °C. ^c Isolated yields in %.

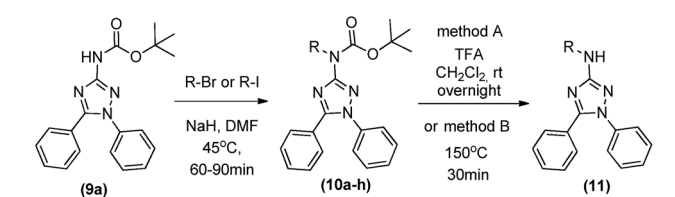


deprotection has been well controlled, based on the temperature as standardized for **6a** and **9a** (Table 3). Also, analysing the reactional yields we could not identify a clear influence of electronic effects of substituents on the cyclocondensations, except for the 4-methoxy group that furnished the lowest yields for both **6b** and **9b** (Table 3).

Finally, as a goal of our medicinal chemistry development program, we decided to explore *N*-alkylations on the 3-amino group. First, we tried the methylation of the deprotected 1,5-diphenyl-3-amine-1,2,4 triazole (**6a**) in some conditions, varying the base, temperature, and molar proportion. Curiously, none of these conditions led to the desired alkylated product (results not shown). As we could selective synthesize the protected 1,5-diphenyl-3-amine-1,2,4 triazole (**9a**), this compound was reacted with methyl iodide, NaH and DMF in a borosilicate sealed tube during around 1 h at 45 °C. The consumption of start material was observed and after chromatographic isolation we could obtain the protected *N*-methyl-1,5-diphenyl-3-amine-1,2,4 triazole (**10a**) in 62% (Table 4).

This methodology was applied to other alkylating agents, furnishing the *N*-alkylated products (**10b–h**) in reasonable to good yields (41–82%) (Table 4). Bulky alkylating groups as dibromoethane did not work in this synthesis. For bioactivity analysis, it is not so interesting to use compounds with protecting groups. Thus, we first tried a deprotection of Boc group with TFA in dichloromethane at room temperature, leading to **11a** in 92% yield. After, we proceeded with a one-pot process of methylation and deprotection from the starting material (**9a**). After the total methylation of **9a**, observed by TLC, we heated the reaction to 150 °C for 30 min and we could observe the deprotection of **10a**, furnishing **11** in 59% global yield (2 steps one pot procedure) after chromatographic isolation (Table 4).

Table 4 Synthesis of *N*-alkyl-1,5-diphenyl-3-amine-1,2,4 triazoles (**10** and **11**)



Entry	Comp.	R	Yield ^a
1	10a	–CH ₃	62
2	10b	–CH ₂ CH ₃	65
3	10c	–CH ₂ CH ₂ CH ₃	65
4	10d	–CH ₂ CH(CH ₃) ₂	41
5	10e	–CH ₂ Ph	79
6	10f	–C ₄ H ₈ Br	82
7	10g	–C ₅ H ₁₀ Br	57
8	10h	–C ₆ H ₁₂ Br	65
9	11	–CH ₃	92 ^b
10	11	–CH ₃	59 ^c

^a Isolated yields in %. ^b Deprotection from **10a**. ^c After one-pot 2 steps procedure from **9a**.

Design and synthesis of triazole cholinesterase inhibitors

The knowledge of neurotransmitter disorders in Alzheimer Disease (AD) has led to the approval of drugs with symptomatic effects.¹⁵

The cholinergic hypothesis of AD states that the degeneration of cholinergic neurons in basal forebrain nuclei causes disorders in the presynaptic cholinergic terminals in the hippocampus and neocortex, regions of extreme importance for memory disorders and other cognitive symptoms.¹⁶ Because of neurodegeneration, the activity of cholinergic neurons and levels of neurotransmitter ACh are reduced and the main approach to improve cholinergic neurotransmission is to increase the availability of ACh by inhibition of cholinesterases.¹⁷

Bear in mind the total control in the synthesis and derivatization of our *N*-alkyl-1,5-diphenyl-3-amine-1,2,4 triazoles and the description of cholinesterase inhibition and neuroprotection of triazine derivative (**12**),¹⁸ we proposed the synthesis of triazoles (**13**). The design was carried out based on the description that multipotent activity of diaryltriazines (**12**) comes from the diaryltriazine moiety and not from the piperazine-ethyl side chain.¹⁸ Thus, we imagined that our 1,5-diphenyl-3-amine-1,2,4 triazoles could be envisaged from a non-classic bioisosterism¹⁹ of ring contraction from diaryltriazines (**12**). And finally, a molecular hybridization²⁰ with the classical drug donepezil (**14**) could furnish the desired triazoles as cholinesterase inhibitors (Fig. 3).

The desired 1,5-diphenyl-3-amine-1,2,4 triazoles (**13a–d**) were obtained in a two-step synthesis (Table 5): (1) a reaction of compounds **10f–i** with 3 equivalents of benzylpiperazine in acetonitrile for 12 h at 60 °C, furnishing products **15a–d** in yields ranging from 66 to 93% after chromatographic purification; and (2) a deprotection of Boc group with TFA in dichloromethane, as above described, leading to desired products **13a–d** in yields ranging from 88 to 94%. In these cases, the thermal deprotection at 150 °C, despite of being faster (around 30–60 min) did not work very well originating some impurities.

Biological profile

The cholinesterase (AChE and BuChE) inhibition activities of the designed triazole derivatives (**13a–d**) and the non-

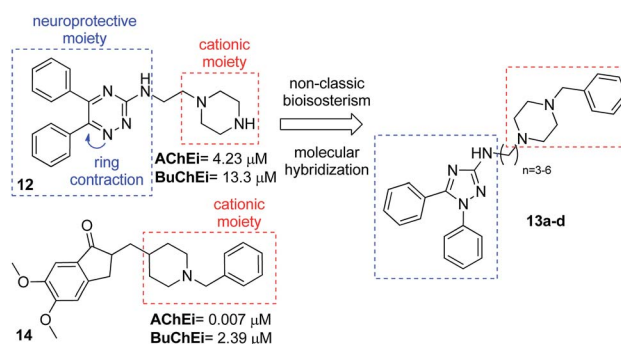
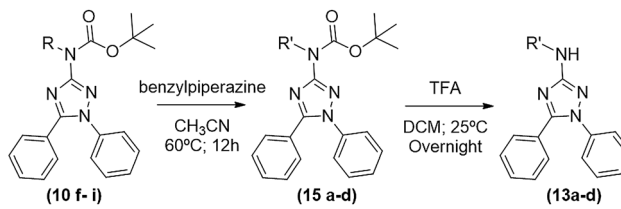


Fig. 3 Structural design of *N*-alkyl-1,5-diphenyl-3-amine-1,2,4 triazoles (**13a–d**) as cholinesterase inhibitors.



Table 5 Synthesis of *N*-alkyl-1,5-diphenyl-3-amine-1,2,4 triazoles (15 and 13)



Comp.	R'	Yield ^a
15a	-C ₃ H ₆ -PipBn	66
15b	-C ₄ H ₈ -PipBn	86
15c	-C ₅ H ₁₀ -PipBn	93
15d	-C ₆ H ₁₂ -PipBn	81
13a	-C ₃ H ₆ -PipBn	94
13b	-C ₄ H ₈ -PipBn	95
13c	-C ₅ H ₁₀ -PipBn	88
13d	-C ₆ H ₁₂ -PipBn	90

^a Isolated yields in %.

substituted triazole **6a** were determined by the Ellman's method²¹ using donepezil as reference compound.

As depicted in Table 6, compounds (**13a–d**) presented good inhibitory activities against AChE with IC₅₀ values varying from 1.14 to 11.00 μM for compounds **13a** and **13c** respectively.

The inhibition profile of triazoles (**13a–d**) against AChE was quite similar of that related in the literature with a regular decreasing of activity with the increasing of the number of methylene spacers. Compound **13a**, which has the smallest methylene chain, was the most potent compound. Curiously, compound **13c** (IC₅₀ = 11.00 μM), which has five methylenes in the spacer chain, was an exception, being considerably less potent than its upper homolog (**13d**, IC₅₀ = 5.22 μM). This result may represent a tendency of an alternating, or serrated, curve as the carbon spacer chain increases. Sometimes this curve can occur in a homologous series when variations in activity are observed according to whether the number of carbons is even or odd, because of the different 3D disposition of attached functional groups. This difference in activity when plotted *versus* the methylene spacer number originate this "serrated" profile. Interestingly serrated curve variations for AChE inhibitory

Table 6 Cholinesterase inhibition of compounds (**13a–d**)

Compound	AChE IC ₅₀ ^{a,b} (μM)	BuChE IC ₅₀ ^{a,c} (μM)
13a	1.14 ± 0.031	1.79 ± 0.060
13b	3.79 ± 0.061	1.63 ± 0.111
13c	11.00 ± 0.251	1.65 ± 0.059
13d	5.22 ± 0.188	2.21 ± 0.068
6a	NA ^d	NA ^d
Donepezil	0.007 ± 0.0002	2.39 ± 0.105

^a Concentration required for 50% inhibition of ChEs, data were shown in mean ± SD of triplicate independent experiments. ^b AChE from electric eel. ^c BuChE from horse serum. ^d NA – not active, inhibition < 20% at 30 μM.

activity were also observed in the literature for donepezil analogues.²²

Additionally, all the tested triazoles (**13a–d**) were also capable of inhibiting BuChE (Table 6) with equipotent IC₅₀ values, ranging from 1.63 to 2.21 μM (compounds **13b** and **13d** respectively). These potency values were comparable to the reference compound donepezil (IC₅₀ = 2.39 μM). Additional results obtained by kinetic study with derivative **13a**, revealed a mixed-type inhibition with a very similar non-competitive constant (K'_i) for AChE ($K'_i = 1.29$ μM) and BuChE ($K'_i = 1.29$ μM). Additionally, the competitive inhibition constant (K_i) for this compound was only 1.7 times higher for BuChE ($K_i = 0.62$ μM) compared to acetylcholinesterase ($K_i = 0.36$ μM) (Fig. 4). The obtained results suggest that the assayed triazoles (**13a–d**) presented good mixed-type inhibition potency, as the prototypal triazine (**12**), but without showing selectivity between AChE and BuChE enzymes. Nevertheless, with the molecular understanding of how triazoles interact with cholinesterases, further modifications could lead to a better selective profile.

Furthermore, the planned derivatizations were correct and important for the activity since **6a** had no significant cholinesterase inhibition at 30 μM.

Molecular modeling

All four scoring functions available in GOLD 5.6 were able to produce docking poses in the redocking of *N,N'*-di-1,2,3,4-tetrahydroacridin-9-yl-pentane-1,5-diamine with RMSD values lower than 1.00 Å. GoldScore²³ was the only function for which the pose with the lowest RMSD value (0.62 Å) was also the pose with the highest docking score, so it was chosen for the subsequent docking procedure.

In the GOLD program, the docking functions yield the "fitness scores", which are dimensionless values. The score values are a guide of how good the docking pose is, with a higher score indicating a better interaction between the ligand and the binding site. All compounds were predicted to interact effectively with EeAChE and EcBuChE using the GoldScore fitness score function.

Comparing compounds **13a** and **13c**, which presented the greater difference in activity as EeAChE inhibitors, it was obtained a better fitness score for **13a** using the 1C2O EeAChE structure and the ligands protonated at the N atom attached to

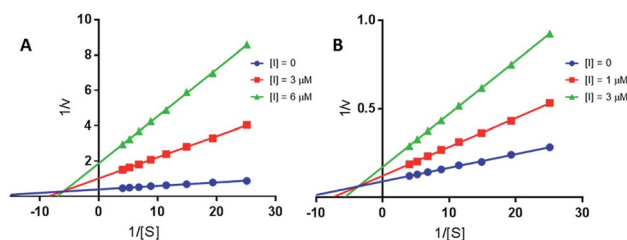


Fig. 4 Lineweaver–Burk plots of EeAChE (A) and EcBuChE (B) inhibition kinetics of compound **13a**. Inset: concentrations used for **13a** are depicted with [I] graphic symbol.



the benzyl group (Table 7). The fitness score was higher for compound **13c** but closer to that of compound **13a** (both with the same protonation mode used for the EeAChE docking) when they were docked in the EcBuChE model. All these results are in qualitative accordance with the experimental activity data.

Similarly to what was observed in the complex between *N,N'*-di-1,2,3,4-tetrahydroacridin-9-yl-pentane-1,5-diamine in *T. californica* AChE by Rydberg and collaborators²⁴ and also in accordance with our previous results,²⁵ it could be observed that the present compounds were able to spread from the peripheral site to the active site inside the EeAChE structure, completely occupying the gorge connecting them. This is in accordance with the experimental results that showed a mixed-type inhibition for these compounds.

In Fig. 5, it is presented a superposition of the docking poses of the strongest (**13a**) and the weakest (**13c**) EeAChE inhibitors of the series. It can be observed that in the active site, the phenyl substituents of the triazole ring interact by means of T-stacking interactions with Trp86 for both inhibitors, in a similar way as described for the prototype **12**.¹⁸ Most of interactions involve the side chains of aromatic rings, including some located at the gorge, which is lined with aromatic residues. However, conversely from **12**, one of these residues (Tyr124) is donating a hydrogen bond to one of the N atoms of the triazole ring in our compounds.

The main difference between the interaction modes of these compounds (**13a** and **13c**) occur at the peripheral binding site (PAS). Because of its smaller spacer chain, the protonated piperazine ring of compound **13a** is located exactly over the Trp286 side chain, which enables the formation of a strong cation- π interaction. However, because compound **13c** side chain is two methylenes longer, a strong interaction between its protonated piperazine ring and Trp286 is impaired, which explains its weaker interaction with the enzyme. Worth of note, this interaction differs from others cholinesterase inhibitors bearing cationic groups like piperazine and piperidine, once these groups normally interact with the catalytic site (CAS) instead of PAS like ours.

To better quantify the effect of the difference in the interaction pattern with the PAS, we implemented PM6 calculations for **13a** and **13c** at the docking geometries of the inhibitor/Trp286 pairs.

From the resulting enthalpies of formation (ΔH_f), the ΔH_f of the corresponding inhibitor and of the Trp286 residue were subtracted, resulting in the interaction enthalpy (ΔH_{int}) between each inhibitor and the Trp286 residue. For the **13c**/Trp286 pair, the calculated ΔH_{int} was $-41.5 \text{ kJ mol}^{-1}$, whereas for the **13a**/Trp286 pair, ΔH_{int} was $-59.5 \text{ kJ mol}^{-1}$. With these values, it is clear how the differences in the interaction

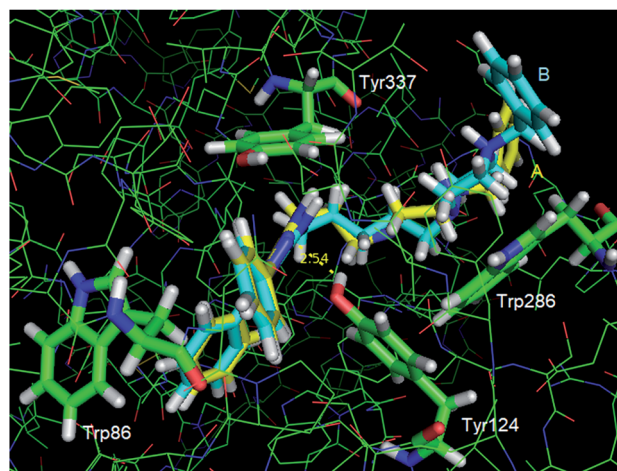


Fig. 5 Superposition of the interaction poses of compounds **13a** (A, carbon atoms in yellow) and **13b** (B, carbon atoms cyan) with EeAChE obtained by molecular docking (Goldscore function). Color code: oxygen atoms, red; nitrogen atoms, blue; hydrogen atoms, white; carbon atoms, green. Dashed yellow line: hydrogen bond distance (Å). Figure generated with PyMol 0.99 (DeLano Scientific LLC).

geometries favors the interaction with the ligand with a shorter spacer, **13a**.

Predicted ADMET profile analysis

To accede the drugability of tested triazoles, we proceeded with *in silico* evaluations that showed a good ADMET profile for these compounds. Parameters as topological polar surface area (TPSA), consensus log *P*, log *S*, human intestinal absorption (HIA), blood brain barrier permeation (BBB), and P-glycoprotein (P-gP) substrate and drug-likeness profile were analyzed (ESI[†]).²⁶ TPSA value was calculated as 49.22 \AA^2 and consensus log *P* ranged from 4.27 to 5.18. The moderate polarity and relative lipophilic characteristics put our compounds in the yellow compartment of BOILED-Egg model (Fig. 6), having a high probability to gastrointestinal absorption and access to the CNS,²⁷ which is fundamental for the distribution of

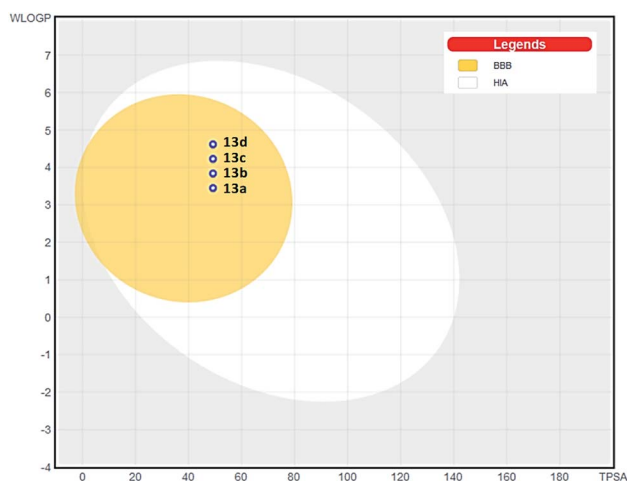


Fig. 6 BOILED-Egg ADMET model²⁷ for triazole compounds **13a**–**d**. (HIA) gastrointestinal absorption; (BBB) brain penetration.

Table 7 Fitness scores (Goldscore)* obtained by molecular docking in EeAChE and EcBuChE

Ligand	EeAChE	EcBuChE
13a	83.7	69.7
13c	79.7	71.5



central-acting molecules. Additionally, the most potent compound **13a** presented a good drug-likeness profile according to Lipinski,²⁸ Veber²⁹ and Egan³⁰ rules.

Conclusions

We could develop an efficient and regioselective one-pot synthesis protocol for obtaining *N*-protected or *N*-deprotected functionalized 1,5-diaryl-3-amino-1,2,4-triazoles starting from *N*-acyl-*N*-Boc-carbamidothioates. This protocol demonstrated that microwave irradiation was very useful reducing reaction times to up to 1 h and presenting yields ranging from 50 to 84%. This chemistry summed to bioisosteric and molecular hybridization techniques allowed us to discover a new series of compounds able to inhibit cholinesterases (without selectivity) with good IC₅₀ of up to 1 μM acting by a mixed-type way. Molecular modelling evaluations demonstrated the importance of phenyl substituents as well as the triazole ring to the interaction with CAS site of AChE, showing potential for this class of compounds as new scaffolds for this biological activity.

Experimental

Materials and instruments

All chemicals were purchased from commercial suppliers and used without further purification. The ¹H and ¹³C NMR spectra were recorded using a 400 MHz or 500 MHz Bruker Avance spectrometer (AC-400 or AC-500), using DMSO-*d*₆ or CDCl₃ and TMS as an internal standard. The melting points recorded are uncorrected. Elemental analyzes were carried out on a Thermo Scientific Flash EA 1112 Series CHN-Analyzer. A Biotage Initiator 2 Reactor was used for microwave reactions using an internal IR temperature probe.

All commercial reagents were used without prior purification. Reactions were monitored by thin layer chromatography (TLC) using silica gel plates and visualized in UV light (254 nm and 365 nm). The multiplicities were called sl (singlet), d (doublet), t (triplet), q (quartet), dd (double doublet) and m (multiplet).

Synthesis of *S*-methyl-urea (**1**)

Methyl iodide (0.82 mL, 13.13 mmol) was added in a sealed tube containing thiourea (0.50 g, 6.56 mmol) in methanol (5 mL). The mixture was stirred at 65 °C for 2 hours. At the end of the reaction the mixture was concentrated on a rotary evaporator to give 1.42 g of a brown solid in 99% yield. ¹H NMR (500 MHz, DMSO) (δ ppm): 2.58 (s, 3H); DEPT-Q (125 MHz, DMSO) (δ ppm): 171.09, 13.55.

Synthesis of 2,5-dioxopyrrolidine-1-benzoate

Benzoic acid (0.10 g, 0.82 mmol), *N,N'*-dicyclohexylcarbodiimide (DCC) (0.22 g, 0.82 mmol) and *N*-hydroxysuccinimide (0.12 g, 0.82 mmol) were solubilized in THF (10 mL). The resulted solution was kept under stirring at room temperature for 20 hours. Reaction mixture was filtered and evaporated on

a rotary evaporator to give 216 mg of a beige solid in 71% yield that was used without any further purification.

Synthesis of *S*-methyl-*N*-benzoyl-isothiourea (**3**)

To a solution of methylisothiourea (0.06 g, 0.28 mmol) in saturated sodium bicarbonate (2 mL) was slowly added under stirring a solution of 2,5-dioxopyrrolidine-1-benzoate (0.06 g, 0.28 mmol) in dichloromethane (10 mL). The reaction mixture was stirred at room temperature for 18 hours. After its completion, the reaction was diluted in dichloromethane (20 mL) and washed with water (3 × 10 mL). The organic phase was dried over anhydrous sodium sulphate and concentrated on a rotary evaporator to give a white amorphous solid in 72% yield. ¹H NMR (400 MHz, CDCl₃) (δ ppm): 8.28–8.26 (d, 2H), 7.53–7.51 (m, 1H), 7.45–7.41 (m, 2H), 2.63 (sl, 3H); DEPT-Q (100 MHz, CDCl₃) (δ ppm): 137.27, 132.03 (2x), 129.68 (2x), 128.04, 13.84.

General procedure for 3-amine-1,2,4 triazoles preparation (**5** and **6a**) from **3**

In a sealed borosilicate tube, methyl *N'*-benzoylcarbamidothioate (**3**) (1 eq.) and phenylhydrazine (**4**) (1.1 eq.) were solubilized in the correspondent solvent (2 mL). The reaction mixture was stirred at temperature and time determined in Table 1. After completion of reaction the slurry was diluted with ethyl acetate (20 mL) and partitioned with water (10 mL). The organic phase was dried over anhydrous sodium sulphate and concentrated on a rotary evaporator. The products were purified by silica gel column chromatography (FLASH Chromatography System – Biotage), using an ultra-10 g snap column (*n*-hexane: ethyl acetate, 5–75% gradient elution).

1,3-diphenyl-1,2,4-triazol-5-amine (**5**)

Brown solid; 13% yield; mp = 159–160 °C; ¹H NMR (500 MHz, CDCl₃) (δ ppm): 8.06–8.06 (d, 2H), 7.64–7.62 (d, 2H), 7.56–7.54 (t, 2H), 7.44–7.40 (m, 5H), 4.80 (s, 2H); DEPT-Q (125 MHz, CDCl₃) (δ ppm): 159.28, 153.92, 136.81, 133.35, 130.76, 129.88, 129.21, 128.50, 128.23, 127.39, 126.16 (2X), 123.45 (2X). Elemental analysis calcd (%) for C₁₄H₁₂N₄: C, 71.17; H, 5.12; N, 23.71; found: C 71.05, H 5.22, N 23.63.

1,5-Diphenyl-1,2,4-triazol-3-amine (**6a**)

Brown solid; 75% yield; mp = 150–152 °C; ¹H NMR (400 MHz, CDCl₃) (δ ppm): 7.47–7.45 (d, 2H), 7.39–7.32 (m, 8H), 4.27 (sl, 2H); DEPT-Q (100 MHz, CDCl₃) (δ ppm): 162.67, 153.09, 138.28, 129.85, 129.22 (2x), 128.74 (2x), 128.46 (2x), 128.28, 128.04, 125.18 (2x). Elemental analysis calcd (%) for C₁₄H₁₂N₄: C, 71.17; H, 5.12; N, 23.71; found: C 71.21, H 5.35, N 23.48.

General procedure for synthesis of 3-amine-1,2,4-triazoles (**6b–6f**) from **7a–d**

In a sealed borosilicate tube containing Boc-*S*-methyl-*N*-benzoyl-isothiourea intermediates **7a–d** (1 eq.) in DMF (2 mL) it was added the corresponding hydrazine (1.1 eq.). The reaction was carried out in microwave irradiation at 150 °C for 60



minutes. After the end of the reaction, the slurry was partitioned between ethyl acetate (20 mL) and water (10 mL). The organic phase was dried over anhydrous sodium sulphate and concentrated on a rotary evaporator. Products were separated by FLASH Chromatography System (Biotage), using an ultra-10 g snap column (*n*-hexane: ethyl acetate, 5–75% gradient elution).

1,5-Diphenyl-1,2,4-triazol-3-amine (6a)

Brown solid; 82% yield; spectral data described before.

5-(4-methoxyphenyl)-1-phenyl-1,2,4-triazol-3-amine (6b)

Brown solid; 47% yield, mp = 198–200 °C; ¹H NMR (500 MHz, CDCl₃) (δ ppm): 7.44–7.37 (m, 7H), 6.94–6.93 (d, 2H), 6.86–6.84 (d, 2H), 3.82 (sl, 3H); DEPT-Q (125 MHz, CDCl₃) (δ ppm): 161.23, 153.04, 130.42, 129.48, 129.20, 129.06, 125.50, 114.06, 113.35, 55.34. Elemental analysis calcd (%) for C₁₅H₁₆N₄O: C, 67.65; H, 5.30; N, 21.04; found: C 67.62, H 5.21, N 21.28.

5-(4-chlorophenyl)-1-phenyl-1,2,4-triazol-3-amine (6c)

Beige solid; 68% yield, mp = 151–153 °C; ¹H NMR (400 MHz, CDCl₃) (δ ppm): 7.43–7.42 (m, 5H), 7.33–7.31 (m, 4H); DEPT-Q (100 MHz, CDCl₃) (δ ppm): 161.76, 151.26, 137.66, 136.53, 130.01 (2X), 128.98 (2X), 128.90, 125.43, 125.20 (2X), 101.30. Elemental analysis calcd (%) for C₁₄H₁₁N₄Cl: C, 62.11; H, 4.10; N, 20.70; found: C 62.00, H 4.31, N 20.63.

5-(4-nitrophenyl)-1-phenyl-1,2,4-triazol-3-amine (6d)

Yellow solid; 52% yield, mp = 202–204 °C; ¹H NMR (500 MHz, CDCl₃) (δ ppm): 8.19–8.17 (d, 2H), 7.65–7.64 (d, 2H), 7.45 (sl, 3H), 7.32 (m, 2H), 4.33 (sl, 2H); DEPT-Q (125 MHz, CDCl₃) (δ ppm): 162.97, 150.72, 148.25, 137.64, 133.77, 129.68 (2X), 129.55 (2X), 129.17, 125.32 (2X), 123.73 (2X). Elemental analysis calcd (%) for C₁₄H₁₁N₅O₂: C, 59.78; H, 3.94; N, 24.90; found: C 59.55, H 4.02, N 24.95.

1-(4-nitrophenyl)-5-phenyl-1,2,4-triazol-3-amine (6e)

Brown solid; 73% yield, mp = 173–176 °C; ¹H NMR (500 MHz, CDCl₃) (δ ppm): 8.27–8.26 (d, 2H), 7.54–7.49 (m, 5H), 7.45–7.43 (m, 2H), 4.99 (sl, 2H); DEPT-Q (125 MHz, CDCl₃) (δ ppm): 160.70, 146.97, 142.07, 131.72, 129.35 (2X), 128.95 (2X), 125.25, 125.00 (2X), 124.93 (2X). Elemental analysis calcd (%) for C₁₄H₁₁N₅O₂: C, 59.78; H, 3.94; N, 24.90; found: C 59.43, H 4.14, N 24.78.

1-(4-(methylsulfonyl)phenyl)-5-phenyl-1,2,4-triazol-3-amine (6f)

Brown solid; 69% yield, mp = 213–215 °C; ¹H NMR (500 MHz, CDCl₃) (δ ppm): 7.94–7.92 (d, 2H), 7.53 (d, 2H), 7.45 (m, 3H), 7.42–7.39 (m, 2H), 4.38 (sl, 2H), 3.08 (sl, 3H); DEPT-Q (125 MHz, CDCl₃) (δ ppm): 163.04, 153.84, 142.25, 139.25, 130.60 (2X), 128.94, 128.80 (2X), 128.60 (2X), 127.56, 124.78 (2X), 44.46. Elemental analysis calcd (%) for C₁₅H₁₄N₄O₂S: C, 57.31; H, 4.49; N, 17.82; found: C 57.32, H 4.54, N 17.66.

General synthesis of compounds (7a–7d)

In a flask containing benzoic acid (1 eq.) and dichloromethane (5 mL) it was added oxalyl chloride (4 eq.) and catalytic amount of dimethylformamide (DMF). After total consumption of the correspondent carboxylic acid, the reaction was concentrated on a rotary evaporator and diluted with dichloromethane (5 mL). This solution was added dropwise to another solution containing the protected *S*-metil-isothiurea (**8**) (1 eq.) and triethylamine (2 eq.) in dichloromethane (10 mL) and kept under stirring overnight. Then, mixture was diluted with dichloromethane (20 mL) and washed with aqueous sodium bicarbonate 10% (3 × 10 mL). Organic phase was dried over sodium sulphate and evaporated on a rotary evaporator.

tert-Butyl(benzamido(methylthio)methylene)carbamate (7a)

White solid; 70% yield; ¹H NMR (500 MHz, CDCl₃) (δ ppm): 8.29–8.28 (d, 2H), 7.56–7.46 (dd, 3H), 2.59 (sl, 3H), 1.54 (sl, 9H); DEPT-Q (125 MHz, CDCl₃) (δ ppm): 172.03, 132.81, 130.12 (2X), 128.25 (2X), 27.98 (3X), 14.92. Elemental analysis calcd (%) for C₁₄H₁₈N₂O₃S: C, 57.12; H, 6.16; N, 9.52; found: C 56.89, H 6.38, N 9.33.

tert-Butyl((4-methoxybenzamido)(methylthio)methylene)carbamate (7b)

White solid; 68% yield; ¹H NMR (400 MHz, CDCl₃) (δ ppm): 8.11–8.09 (d, 2H), 7.06–7.04 (d, 2H), 3.85 (sl, 3H), 2.49 (sl, 3H), 1.46 (sl, 9H). DEPT-Q (100 MHz, CDCl₃) (δ ppm): 171.00, 163.44, 151.12, 132.32 (2X), 129.31, 113.49 (2X), 83.26, 55.43, 27.98 (3X), 14.86. Elemental analysis calcd (%) for C₁₅H₂₀N₂O₄S: C, 55.54; H, 6.21; N, 8.64; found: C 55.72, H 6.29, N 8.77.

tert-Butyl(4-chlorobenzamido(methylthio)methylene)carbamate (7c)

White solid; 63% yield; ¹H NMR (500 MHz, CDCl₃) (δ ppm): 12.54 (sl, 1H), 8.22–8.20 (d, 2H), 7.43–7.41 (d, 2H), 2.58 (sl, 3H), 1.53 (sl, 9H); DEPT-Q (125 MHz, CDCl₃) (δ ppm): 174.93, 172.63, 150.95, 139.17, 135.14, 131.48 (2X), 128.55 (2X), 83.64, 27.98 (3X), 14.97. Elemental analysis calcd (%) for C₁₄H₁₇ClN₂O₃S: C, 51.14; H, 5.21; N, 8.52; found: C 51.00, H 5.39, N 8.41.

tert-Butyl((4-nitrobenzamido)(methylthio)methylene)carbamate (7d)

White solid; 58% yield; ¹H NMR (500 MHz, CDCl₃) (δ ppm): 7.04 (s, 1H); 2.51 (s, 3H); 1.52 ppm (s, 9H); DEPT-Q (125 MHz, CDCl₃) (δ ppm): 174.28, 173.68, 150.76, 150.21, 142.03, 130.95 (2X), 123.27 (2X), 84.06, 27.95 (3X), 15.12. Elemental analysis calcd (%) for C₁₄H₁₇N₃O₅S: C, 49.55; H, 5.05; N, 12.38; found: C 49.21, H 5.24, N 12.02.

tert-Butyl(1*H*-pyrrole-2-carboxamido(methylthio)-methylene)carbamate (7e)

White solid; 80% yield; ¹H NMR (500 MHz, CDCl₃) (δ ppm): 12.49 (s, 1H), 9.55 (s, 1H), 7.10 (s, 1H), 7.02 (s, 1H), 6.30 ppm (s, 1H), 2.52 (s, 3H), 1.51 (s, 9H). DEPT-Q (125 MHz, CDCl₃) (δ



ppm): 170.5, 151.1, 130.5, 116.8, 110.9, 83.5, 27.9, 14.6. Elemental analysis calcd (%) for $C_{12}H_{17}N_3O_3S$: C, 50.87; H, 6.05; N, 14.83; found: C 50.71, H 5.98, N 14.96.

***tert*-Butyl(4,5-dibromo-1*H*-pyrrole-2-carboxamido(methylthio)methylene)carbamate (7f)**

White solid; 69% yield; 1H NMR (500 MHz, $CDCl_3$) (δ ppm): 12.53 (sl, 1H), 8.43–8.42 (d, 2H), 8.30–8.28 (d, 2H), 2.61 (sl, 3H), 1.55 (sl, 9H); DEPT-Q (125 MHz, $CDCl_3$) (δ ppm): 119.3; 84.0; 28.0; 15.1. Elemental analysis calcd (%) for $C_{12}H_{15}Br_2N_3O_3S$: C, 32.67; H, 3.43; N, 9.53; found: C 32.38, H 3.64, N 9.48.

Synthesis of *tert*-butyl [amine(methylthio)methylene] carbamate (8)

In a flask containing methyl isothiourea (1 g, 4.58 mmol), dichloromethane (10 mL) and triethylamine (639 μ L, 4.58 mmol), in an ice-bath, it was slowly added a solution of di-*tert*-butyl dicarbonate (Boc-O-Boc) (0.5 g, 2.29 mmol) in dichloromethane (5 mL). Then, ice bath was removed and reaction was left under stirring overnight at room temperature. After consumption of reactants, the reaction mixture was diluted with dichloromethane (15 mL), washed with water (2 \times 10 mL), dried over sodium sulphate and concentrated on a rotary evaporator. A white solid product was obtained in 86% yield and used without any further purification.

1H NMR (500 MHz, DMSO) (δ ppm): 8.58 (sl, 2H), 2.32 (sl, 3H), 1.41 (sl, 9H); DEPT-Q (125 MHz, DMSO) (δ ppm): 171.87, 160.98, 78.11, 26.17 (3X), 13.13.

Synthesis of compounds 9a–9e

In a sealed borosilicate tube containing triazole (7a–7f) (1 eq.) in 2 mL of acetonitrile, it was added the corresponding hydrazine (1.1 eq.). Reaction was stirred at 100 $^\circ$ C for 40 minutes as shown in Table 3. After the end of the reaction, the reactional slurry was partitioned between ethyl acetate (20 mL) and water (10 mL). The organic phase was dried over anhydrous sodium sulphate and concentrated on a rotary evaporator. The products were separated with a FLASH Chromatography System (Biotage), using an ultra-10 g snap column (*n*-hexane: ethyl acetate, 5–75% gradient elution).

***tert*-Butyl(1,5-diphenyl-1,2,4-triazol-3-yl)carbamate (9a)**

Brown solid; 87% yield, mp = 147–149 $^\circ$ C; 1H NMR (400 MHz, $CDCl_3$) (δ ppm): 7.49 (m, 3H), 7.39 (sl, 6H), 7.34–7.32 (d, 2H), 1.52 (s, 9H); DEPT-Q (100 MHz, $CDCl_3$) (δ ppm): 156.33, 153.05, 151.32, 138.08, 130.11, 129.23 (2X), 128.93 (2X), 128.50 (2X), 125.75 (2X), 81.34, 28.21 (3X). Elemental analysis calcd (%) for $C_{19}H_{20}N_4O_2$: C, 67.84; H, 5.99; N, 16.66; found: C 68.02, H 6.07, N 16.62.

***tert*-Butyl(5-(4-methoxyphenyl)-1-phenyl-1,2,4-triazol-3-yl) carbamate (9b)**

Brown solid; 62% yield, mp = 164–167 $^\circ$ C; 1H NMR (400 MHz, $CDCl_3$) (δ ppm): 7.59 (sl, 1H), 7.43–7.39 (m, 7H), 6.84–6.82 (d, 2H), 3.81 (s, 3H), 1.51 (s, 9H); DEPT-Q (100 MHz, $CDCl_3$) (δ ppm):

161.01, 155.94, 151.28, 138.11, 130.43 (2X), 129.25 (2X), 128.77, 125.82 (2X), 113.94 (2X), 81.34, 55.31, 28.18 (3X). Elemental analysis calcd (%) for $C_{20}H_{22}N_4O_3$: C, 65.56; H, 6.05; N, 15.29; found: C 65.90, H 6.07, N 14.99.

***tert*-Butyl(5-(4-chlorophenyl)-1-phenyl-1,2,4-triazol-3-yl) carbamate (9c)**

White solid; 71% yield, mp = 140–142 $^\circ$ C; 1H NMR (400 MHz, $CDCl_3$) (δ ppm): 7.94 (sl, 1H), 7.43–7.41 (m, 4H), 7.38 (d, 2H), 7.31–7.25 (m, 3H), 1.49 (s, 9H); DEPT-Q (100 MHz, $CDCl_3$) (δ ppm): 156.47, 151.93, 151.33, 137.75, 136.37, 130.18 (2X), 129.38 (2X), 129.05 (2X), 128.82 (2X), 125.74, 125.78, 81.37, 28.14 (3X). Elemental analysis calcd (%) for $C_{19}H_{19}ClN_4O_2$: C, 61.54; H, 5.16; N, 15.11; found: C 61.23, H 5.34, N 14.82.

***tert*-Butyl(5-(4-nitrophenyl)-1-phenyl-1,2,4-triazol-3-yl) carbamate (9d)**

White solid; 80% yield, mp = 166–168 $^\circ$ C; 1H NMR (400 MHz, $CDCl_3$) (δ ppm): 8.19–8.17 (d, 2H), 7.69–7.66 (d, 2H), 7.47–7.45 (m, 3H), 7.39–7.36 (m, 3H), 1.54 (s, 9H); DEPT-Q (100 MHz, $CDCl_3$) (δ -ppm): 156.71, 151.10, 148.41, 137.40, 133.22, 129.78 (2X), 129.67 (2X), 129.62, 125.79 (2X), 123.72 (2X), 81.76, 28.18 (3X). Elemental analysis calcd (%) for $C_{19}H_{19}N_5O_4$: C, 59.84; H, 5.02; N, 18.36; found: C 59.78, H 5.12, N 18.21.

***tert*-Butyl (1-(4-nitrophenyl)-5-phenyl-1,2,4-triazol-3-yl) carbamate (9e)**

Brown solid; 61% yield, mp = 147–150 $^\circ$ C; 1H NMR (400 MHz, DMSO) (δ ppm): 10.12 (s, 1H), 8.35–8.33 (d, 2H), 7.65 (d, 2H), 7.49–7.47 (m, 5H), 1.49 (s, 9H); DEPT-Q (100 MHz, DMSO) (δ ppm): 157.53, 153.88, 152.38, 147.19, 143.08, 131.21, 129.52 (2X), 127.85, 126.48 (2X), 125.52 (2X), 80.19, 28.61 (3X). Elemental analysis calcd (%) for $C_{19}H_{19}N_5O_4$: C, 59.84; H, 5.02; N, 18.36; found: C 59.95, H 5.01, N 18.14.

***tert*-Butyl (1-(4-(methylsulfonyl)phenyl)-5-phenyl-1,2,4-triazol-3-yl)carbamate (9f)**

Brown solid; 84% yield, mp = 179–181 $^\circ$ C; 1H NMR (400 MHz, $CDCl_3$) (δ ppm): 7.96–7.94 (d, 2H), 7.90 (s, 1H), 7.61–7.60 (d, 2H), 7.46 (m, 3H), 7.41–7.38 (m, 2H), 3.07 (s, 3H), 1.50 (s, 9H); DEPT-Q (100 MHz, $CDCl_3$) (δ ppm): 156.94, 153.56, 151.12, 142.09, 140.00, 130.85, 128.96 (2X), 128.64 (2X), 126.82, 125.73 (2X), 81.66, 44.46, 28.11 (3X). Elemental analysis calcd (%) for $C_{20}H_{22}N_4O_4S$: C, 57.96; H, 5.35; N, 13.52; found: C 57.59, H 5.55, N 13.28.

***tert*-Butyl (1-phenyl-5-(1*H*-pyrrol-2-yl)-1-phenyl-1*H*-1,2,4-triazol-3-yl)carbamate (9g)**

Brown solid; 90% yield, mp = 170–172 $^\circ$ C; 1H NMR (500 MHz, $CDCl_3$) (δ ppm): 12.49 (s, 1H), 9.55 (s, 1H), 7.10 (s, 1H), 7.02 (s, 1H), 6.30 ppm (s, 1H), 2.52 (s, 3H), 1.51 (s, 9H). DEPT-Q (125 MHz, $CDCl_3$) (δ ppm): 170.5, 151.1, 130.5, 116.8, 110.9, 83.5, 27.9, 14.6. Elemental analysis calcd (%) for $C_{17}H_{19}N_5O_2$: C, 62.75; H, 5.89; N, 21.52; found: C 62.79, H 5.95, N 21.38.



***tert*-Butyl (5-(4,5-dibromo-1*H*-pyrrol-2-yl)-1-phenyl-1*H*-1,2,4-triazol-3-yl)carbamate (9h)**

Brown solid; 79% yield; ^1H NMR (500 MHz, CDCl_3) (δ ppm): 12.98 (sl, 1H), 9.77 (sl, 1H), 7.59–7.48 (m, 5H), 5.65 (s, 1H), 1.45 (s, 9H). DEPT-Q (125 MHz, CDCl_3) (δ ppm): 155.9, 145.9, 137.5, 130.3, 129.8, 126.7, 120.2, 114.0, 105.5, 100.0, 28.5. Elemental analysis calcd (%) for $\text{C}_{17}\text{H}_{17}\text{Br}_2\text{N}_5\text{O}_2$: C, 42.26; H, 3.55; N, 14.49; found: C 42.13, H 3.58, N 14.25.

General synthesis of compounds 10a–10h

The corresponding alkyl halide (2 eq.) was added in a sealed borosilicate tube containing triazole **9a** (1 eq.) and sodium hydride (4 eq.) in anhydrous DMF (2 mL). The reaction was stirred at 45 °C for 60–90 minutes. When the end of reaction was determined by TLC (hexane: ethyl acetate 30%), mixture was diluted in 20 mL of ethyl acetate and washed with water (3 × 10 mL). The organic phase was dried over sodium sulphate, concentrated and purified by an isolation with FLASH Chromatography System (Biotage), using an ultra-10 g snap column (*n*-hexane: ethyl acetate, 10–50% gradient elution).

***tert*-Butyl (1,5-diphenyl-1,2,4-triazol-3-yl)(methyl) carbamate (10a)**

Yellow oil; 62% Yield; ^1H NMR (400 MHz, CDCl_3) (δ ppm): 7.50–7.48 (d, 2H), 7.40–7.33 (m, 8H), 3.43 (sl, 3H), 1.55 (sl, 9H); DEPT-Q (100 MHz, CDCl_3) (δ ppm): 160.11, 153.56, 153.11, 137.97, 130.01, 129.28 (2X), 128.91 (2X), 128.47 (2X), 127.64, 125.46 (2X), 81.29, 35.54, 28.26 (3X). Elemental analysis calcd (%) for $\text{C}_{20}\text{H}_{22}\text{N}_4\text{O}_2$: C, 68.55; H, 6.33; N, 15.99; found: C 68.32, H 6.51, N 15.88.

***tert*-Butyl (1,5-diphenyl-1,2,4-triazol-3-yl)(ethyl) carbamate (10b)**

Beige solid; 65% yield, mp = 98–99 °C; ^1H NMR (500 MHz, CDCl_3) (δ ppm): 7.50–7.48 (d, 2H), 7.40–7.31 (m, 8H), 3.91–3.86 (m, 2H), 1.53 (sl, 9H), 1.33–1.30 (t, 3H); DEPT-Q (125 MHz, CDCl_3) (δ ppm): 159.40, 153.34, 137.99, 129.96, 129.24 (2X), 128.91 (2X), 128.44 (2X), 127.70, 125.45 (2X), 80.99, 43.58, 28.28 (2X), 14.07. Elemental analysis calcd (%) for $\text{C}_{21}\text{H}_{24}\text{N}_4\text{O}_2$: C, 69.21; H, 6.64; N, 15.37; found: C 69.00, H 6.68, N 15.49.

***tert*-Butyl (1,5-diphenyl-1,2,4-triazol-3-yl)(propyl) carbamate (10c)**

Beige solid; 65% Yield, mp = 97–99 °C; ^1H NMR (500 MHz, CDCl_3) (δ -ppm): 7.50–7.48 (d, 2H), 7.41–7.32 (m, 8H), 3.80–3.77 (t, 2H), 1.79–1.72 (m, 2H), 1.53 (sl, 9H), 0.98–0.95 (t, 3H); DEPT-Q (125 MHz, CDCl_3) (δ ppm): 159.60, 153.62, 153.18, 130.01, 129.98, 129.26 (2X), 128.94 (2x), 128.46 (2X), 127.73, 125.48 (2X), 80.98, 50.19, 28.29 (3X), 22.09, 11.23. Elemental analysis calcd (%) for $\text{C}_{22}\text{H}_{26}\text{N}_4\text{O}_2$: C, 69.82; H, 6.92; N, 14.80; found: C 69.99, H 6.95, N 14.58.

***tert*-Butyl allyl (1,5-diphenyl-1,2,4-triazol-3-yl) carbamate (10d)**

White solid; 41% yield, mp = 82–84 °C; ^1H NMR (500 MHz, CDCl_3) (δ ppm): 7.49–7.47 (d, 2H), 7.40–7.7.31 (m, 8H), 6.06–5.98 (m, 1H), 5.32–5.15 (dd, 2H), 4.47–4.46 (d, 2H), 1.53 (sl, 9H); DEPT-Q (125 MHz, CDCl_3) (δ ppm): 159.40, 153.20, 153.12, 138.00, 133.85, 129.97, 129.24 (2X), 128.94 (2X), 128.44 (2X), 127.69, 125.50 (2X), 116.61, 81.36, 50.79, 28.24 (3X). Elemental analysis calcd (%) for $\text{C}_{22}\text{H}_{24}\text{N}_4\text{O}_2$: C, 70.19; H, 6.43; N, 14.88; found: C 70.22, H 6.52, N 14.97.

***tert*-Butyl benzyl (1,5-diphenyl-1,2,4-triazol-3-yl) carbamate (10e)**

White solid; 79% yield, mp = 110–113 °C; ^1H NMR (500 MHz, CDCl_3) (δ ppm): 7.48–7.47 (m, 4H), 7.39 (m, 5H), 7.32–7.31 (m, 6H), 7.25–7.23 (m, 1H), 5.10 (sl, 2H), 1.47 (sl, 9H); DEPT-Q (125 MHz, CDCl_3) (δ ppm): 159.68, 153.27, 153.07, 138.52, 137.96, 129.95, 129.21 (2X), 128.91 (2X), 128.42 (2X), 128.18 (2X), 127.66, 126.91, 125.49 (2X), 125.14, 118.96, 112.82, 81.54, 56.52, 51.84, 47.84, 28.16 (3X). Elemental analysis calcd (%) for $\text{C}_{26}\text{H}_{26}\text{N}_4\text{O}_2$: C, 73.22; H, 6.14; N, 13.14; found: C 72.97, H 6.42, N 13.23.

***tert*-Butyl(4-bromobutyl)(1,5-diphenyl-1,2,4-triazol-3-yl) carbamate (10f)**

Brown oil; 82% yield; ^1H NMR (500 MHz, CDCl_3) (δ ppm): 7.50–7.48 (d, 2H), 7.41–7.32 (m, 8H), 3.89–3.87 (t, 2H), 3.48–3.46 (t, 2H), 2.01–1.97 (m, 2H), 1.90–1.87 (m, 2H), 1.54 (sl, 9H); DEPT-Q (125 MHz, CDCl_3) (δ ppm): 159.40, 153.50, 153.30, 137.99, 130.08, 129.33 (2X), 128.96 (2X), 128.53 (2X), 127.66, 125.51 (2X), 81.39, 47.41, 33.51, 29.94, 28.31 (3X), 27.47. Elemental analysis calcd (%) for $\text{C}_{23}\text{H}_{27}\text{BrN}_4\text{O}_2$: C, 58.60; H, 5.77; N, 11.89; found: C 58.55, H 5.84, N 11.68.

***tert*-Butyl(5-bromopentyl)(1,5-diphenyl-1,2,4-triazol-3-yl) carbamate (10g)**

Brown oil; 52% yield; ^1H NMR (400 MHz, CDCl_3) (δ ppm): 7.50–7.48 (d, 2H), 7.41–7.23 (m, 7H), 3.86–3.82 (t, 2H), 3.44–3.40 (t, 2H), 1.94–1.90 (m, 2H), 1.79–1.77 (m, 2H), 1.53 (sl, 9H); DEPT-Q (100 MHz, CDCl_3) (δ ppm): 159.48, 153.49, 153.22, 137.96, 130.03, 129.29 (2X), 128.48 (2X), 127.64, 125.46 (2X), 81.21, 48.13, 33.77, 32.38, 28.29 (3X), 27.88, 25.30. Elemental analysis calcd (%) for $\text{C}_{24}\text{H}_{29}\text{BrN}_4\text{O}_2$: C, 59.38; H, 6.02; N, 11.54; found: C 59.01, H 5.89, N 11.34.

***tert*-Butyl(6-bromohexyl)(1,5-diphenyl-1,2,4-triazol-3-yl) carbamate (10h)**

Brown oil; 65% yield; ^1H NMR (400 MHz, CDCl_3) (δ ppm): 7.50–7.48 (d, 2H), 7.41–7.32 (m, 8H), 3.84–3.81 (t, 2H), 3.42–3.39 (t, 2H), 1.89–1.85 (m, 2H), 1.76–1.75 (m, 2H), 1.53 (sl, 9H); DEPT-Q (100 MHz, CDCl_3) (δ ppm): 159.51, 153.55, 153.21, 137.97, 130.01, 129.29 (2X), 128.93 (2X), 128.48 (2X), 127.66, 125.46 (2X), 101.13, 81.11, 48.28, 33.91, 32.70, 28.51, 28.29 (3X), 27.82, 25.80. Elemental analysis calcd (%) for $\text{C}_{25}\text{H}_{31}\text{BrN}_4\text{O}_2$: C, 60.12; H, 6.26; N, 11.22; found: C 59.86, H 6.43, N 11.17.



General synthesis of compounds 15a–15d

Benzylpiperazine (3 eq.) was added in a sealed borosilicate tube containing triazole **10f–h** (1 eq.) and acetonitrile (2 mL). Reaction was stirred at 60 °C until the end of the reaction, determined by TLC (DCM : methanol 10%). Then, mixture was concentrated and purified by an isolation with FLASH Chromatography System (Biotage), using an ultra-10 g snap column (DCM : methanol, 1–50% gradient elution).

tert-Butyl (3-(4-benzylpiperazin-1-yl)propyl)(1,5-diphenyl-1*H*-1,2,4-triazol-3-yl)carbamate (**15a**)

Brown oil; 66% yield; ¹H NMR (500 MHz, CDCl₃) (δ ppm): 7.47–7.45 (d, 2H), 7.40–7.30 (m, 13H), 3.92–3.89 (t, 2H), 3.61 (s, 2H), 2.81–2.76 (m, 8H), 2.12 (m, 2H), 1.51 (sl, 9H), 1.25 (sl, 2H); DEPT-Q (125 MHz, CDCl₃) (δ ppm): 159.03, 153.43, 153.33, 137.78, 130.09, 129.41 (2X), 129.28 (2X), 128.84 (3X), 128.47 (2X), 128.42 (2X), 127.66, 127.40, 125.39 (2X), 81.59, 62.11, 55.17, 52.07, 50.88, 46.12, 28.21, 24.56. Elemental analysis calcd (%) for C₂₇H₃₅N₅O₂: C, 70.25; H, 7.64; N, 15.17; found: C 69.99, H 7.86, N 15.01.

tert-Butyl (4-(4-benzylpiperazin-1-yl)butyl)(1,5-diphenyl-1*H*-1,2,4-triazol-3-yl)carbamate (**15b**)

Brown oil; 86% yield; ¹H NMR (500 MHz, CDCl₃) (δ ppm): 7.48–7.47 (d, 2H), 7.40–7.31 (m, 12H), 3.83 (m, 2H), 3.56 (s, 2H), 2.69 (m, 7H), 1.78 (m, 4H), 1.51 (sl, 9H), 1.26 (m, 1H), 0.88–0.83 (m, 1H); DEPT-Q (125 MHz, CDCl₃) (δ ppm): 163.24, 137.86, 130.10 (2X), 129.26 (3X), 128.89 (2X), 128.51 (3X), 128.37 (2X), 127.44 (2X), 125.43, 81.35, 62.35, 57.47, 52.29, 51.02, 47.71, 28.26, 26.30 (2X). Elemental analysis calcd (%) for C₂₈H₃₇N₅O₂: C, 70.71; H, 7.84; N, 14.72; found: C 70.56, H 8.01, N 14.58.

tert-Butyl (5-(4-benzylpiperazin-1-yl)pentyl)(1,5-diphenyl-1*H*-1,2,4-triazol-3-yl)carbamate (**15c**)

Brown oil; 93% yield; ¹H NMR (500 MHz, CDCl₃) (δ ppm): 7.48–7.46 (d, 2H), 7.40–7.30 (m, 13H), 3.83–3.80 (t, 2H), 3.61 (s, 2H), 2.86 (m, 6H), 1.89 (m, 2H), 1.76–1.72 (m, 2H), 1.51 (sl, 9H), 1.45–1.42 (m, 2H); DEPT-Q (125 MHz, CDCl₃) (δ ppm): 159.33, 153.58, 153.28, 137.86, 130.06, 129.30, 128.49 (2X), 127.54 (2X), 125.43, 81.25, 61.88, 57.28, 49.58, 47.77, 28.26, 27.94, 23.81. Elemental analysis calcd (%) for C₂₉H₃₉N₅O₂: C, 71.13; H, 8.03; N, 14.30; found: C 70.89, H 8.22, N 14.29.

tert-Butyl (6-(4-benzylpiperazin-1-yl)hexyl)(1,5-diphenyl-1*H*-1,2,4-triazol-3-yl)carbamate (**15d**)

Brown oil; 81% yield; ¹H NMR (500 MHz, CDCl₃) (δ ppm): 7.48–7.47 (d, 2H), 7.40–7.31 (m, 12H), 3.81–3.78 (t, 2H), 3.65–3.57 (m, 2H), 3.88 (m, 2H), 2.95–2.80 (m, 7H), 1.88 (m, 2H), 1.73–1.70 (m, 2H), 1.51 (sl, 9H), 1.41 (m, 4H), 0.94–0.89 (m, 1H); DEPT-Q (125 MHz, CDCl₃) (δ ppm): 159.40, 153.59, 153.26, 137.90, 130.05, 129.30 (2X), 128.90 (2X), 128.80 (2X), 128.56 (2X), 127.59, 125.44 (2X), 81.15, 61.80, 57.21, 48.11, 46.80, 31.50, 29.56, 28.30, 28.27, 26.38, 25.87, 25.27, 22.61, 13.93, 11.80. Elemental analysis calcd (%) for C₃₀H₄₁N₅O₂: C, 71.54; H, 8.20; N, 13.90; found: C 71.30, H 8.45, N 13.71.

General synthesis of compounds (13a–13d)

In a sealed borosilicate tube containing triazole **12a–d** (1 eq.) solubilized dichloromethane (4 mL) in an ice-bath, it was added trifluoroacetic acid (35 eq.). The ice bath was removed and reaction stirred at room temperature overnight. The end of reaction was determined by TLC and saturated sodium bicarbonate solution was added until pH 7 and then, extracted with dichloromethane, dried over sodium sulphate and concentrated on a rotary evaporator.

N-(3-(4-benzylpiperazin-1-yl)propyl)-1,5-diphenyl-1*H*-1,2,4-triazol-3-amine (**13a**)

Brown oil; 94% yield; ¹H NMR (400 MHz, CDCl₃) (δ ppm): 7.45–7.43 (d, 2H), 7.37–7.30 (m, 13H), 3.54 (sl, 2H), 3.44–3.42 (t, 2H), 2.66–2.43 (m, 10H), 1.89–1.84 (m, 2H); DEPT-Q (100 MHz, CDCl₃) (δ ppm): 163.98, 152.82, 138.83, 129.79, 129.23, 128.46, 128.16, 128.11, 127.64, 125.24, 62.21, 57.34, 43.06, 27.53. Elemental analysis calcd (%) for C₂₈H₃₂N₆O₆: C, 74.30; H, 7.13; N, 18.57; found: C 74.15, H 7.39, N 18.28.

N-(4-(4-benzylpiperazin-1-yl)butyl)-1,5-diphenyl-1*H*-1,2,4-triazol-3-amine (**13b**)

Brown oil; 95% yield; ¹H NMR (400 MHz, CDCl₃) (δ ppm): 7.44–7.43 (d, 2H), 7.38–7.30 (m, 13H), 3.60 (sl, 2H), 3.39–3.37 (t, 2H), 2.75 (m, 6H), 1.76–1.70 (m, 10H); DEPT-Q (100 MHz, CDCl₃) (δ ppm): 164.12, 152.79, 138.90, 137.90, 129.70, 129.25, 129.19, 128.76, 128.42, 128.06, 125.25, 62.92, 56.61, 53.14, 52.86, 42.62, 29.67, 26.34. Elemental analysis calcd (%) for C₂₉H₃₄N₆: C, 74.65; H, 7.34; N, 18.01; found: C 74.48, H 7.51, N 17.82.

N-(5-(4-benzylpiperazin-1-yl)pentyl)-1,5-diphenyl-1*H*-1,2,4-triazol-3-amine (**13c**)

Brown oil; 88% yield; ¹H NMR (400 MHz, CDCl₃) (δ ppm): 7.42–7.41 (d, 2H), 7.35–7.29 (m, 13H), 4.82 (m, 1H), 4.69 (m, 1H), 4.32–4.31 (sl, 1H), 3.60 (sl, 2H), 3.37–3.33 (m, 2H), 2.82 (m, 10H), 1.84 (m, 2H), 1.72–1.66 (m, 2H), 1.48–1.42 (m, 2H); DEPT-Q (100 MHz, CDCl₃) (δ ppm): 163.95, 152.75, 138.28, 129.74, 129.20, 128.68, 128.41, 128.11, 128.05, 127.71, 125.22, 61.93, 57.30, 49.95, 43.05, 29.63, 29.21, 24.05. Elemental analysis calcd (%) for C₃₀H₃₆N₆: C, 74.97; H, 7.55; N, 17.48; found: C 74.66, H 7.68, N 17.27.

N-(6-(4-benzylpiperazin-1-yl)hexyl)-1,5-diphenyl-1*H*-1,2,4-triazol-3-amine (**13d**)

Brown oil; 90% yield ¹H NMR (400 MHz, CDCl₃) (δ ppm): 7.45–7.43 (d, 2H), 7.37–7.31 (m, 12H), 4.27 (sl, 1H), 3.54 (sl, 2H), 3.37–3.33 (m, 2H), 2.59–2.50 (m, 10H), 1.67–1.57 (m, 4H), 1.45–1.35 (m, 4H); DEPT-Q (100 MHz, CDCl₃) (δ ppm): 164.11, 152.79, 138.42, 129.76, 129.29, 128.77, 128.46, 128.31, 128.20, 128.12, 127.27, 125.31, 62.73, 58.20, 52.73, 52.07, 43.56, 29.77, 27.11, 26.68, 25.91. Elemental analysis calcd (%) for C₃₁H₃₈N₆: C, 75.27; H, 7.74; N, 16.99; found: C 74.99, H 7.96, N 16.75.



Biological assessment

Anticholinesterase activity assays. The anticholinesterase activity was determined according to adapted Ellman's method.^{21,25} All of the solutions were prepared in 0.02 M Tris-HCl buffer (pH = 7.5), stock solutions of test compounds prepared in DMSO (50 mM), and the experiment conducted in triplicate. To a flat-bottom 96-well transparent plate were added 150 μL of treatment solutions with inhibitors and donepezil at eight different concentrations serially diluted. Negative (without treatment) and vehicle (DMSO, final concentration 0.2% v/v for AChE and 0.8% v/v for BuChE) controls were kept for reference. Following, there were added 60 μL of 5,5'-dithiobis(2-nitrobenzoic acid) (DTNB, Ellman's reagent) at 1.1 mM and 30 μL of electric eel acetylcholinesterase (EeAChE) or equine serum butyrylcholinesterase (EqBuChE) at 0.20 U mL^{-1} in the presence of 1 mg mL^{-1} bovine serum albumin (BSA). Absorbance was then recorded using an iMark plate reader (Bio-Rad) equipped with a $\lambda = 415$ nm light filter and this measure used as a blank reference. After a 10 minute incubation at 30 $^{\circ}\text{C}$, 24 μL of 2.75 mM acetylthiocholine iodide (ACTI) or *S*-butyrylthiocholine iodide (BCTI) were added and the absorbance recorded after a 10 minute incubation at 30 $^{\circ}\text{C}$ at $\lambda = 415$ nm for 3 times within 30 seconds. Enzyme activity was calculated as percentage of untreated control discounting the blank reference. The final inhibitor concentration ranged from 100–0.00001 μM for AChE (dilution factor = 10) and from 400–0.1 μM for BuChE (dilution factor = 4). IC_{50} values were calculated on Graphpad Prism 7.0 using the non-linear regression model for dose-response inhibition.

Enzymatic kinetic study. The enzymatic kinetic of cholinesterase inhibition was determined according to adapted Ellman's method.^{21,25} All of the solutions were prepared in 0.02 M Tris-HCl buffer (pH = 7.5), stock solutions of test compounds prepared in DMSO (50 mM), and the experiment conducted in triplicate. To a flat-bottom 96-well transparent plate were added 150 μL of treatment solutions with inhibitors at two different concentrations distributed in eight sets of triplicates each. Eight sets of untreated triplicates were used as negative control. Following, there were added 60 μL of 5,5'-dithiobis(2-nitrobenzoic acid) (DTNB, Ellman's reagent) at 1.1 mM and 30 μL of electric eel acetylcholinesterase (EeAChE) or equine serum butyrylcholinesterase (EqBuChE) at 0.20 U mL^{-1} in presence of 1 mg mL^{-1} bovine serum albumin (BSA). Absorbance was then recorded using an iMark plate reader (Bio-Rad) equipped with a $\lambda = 415$ nm light filter and this measure used as a blank reference. After 10 minute incubation at room temperature, 24 μL of acetylthiocholine iodide (ACTI) or *S*-butyrylthiocholine iodide (BCTI) at eight concentrations serially diluted (factor = 1.3) from 2.75–0.44 mM (final concentration: 0.25–0.04 mM) were added to all wells and the absorbance recorded after incubation for 0, 5, 10, 15 and 20 minutes at room temperature at $\lambda = 415$ nm. The Lineweaver-Burk reciprocal plots were obtained by plotting a $1/\text{velocity}$ versus $1/[\text{substrate}]$ graph for two different inhibitor concentrations and untreated control. The linear regression of each data-set shows a convergent behaviour, in ways the region to where the curves converge determine

the type of inhibition observed. K_i , K_i' (competitive and non-competitive inhibition constants respectively), K_m (Michaelis-Menten constant) and V_{max} values were calculated with Graphpad Prism 7.0 using the non-linear regression models for enzyme kinetics – inhibition and enzyme Kinect – substrate *vs.* velocity.

Molecular modeling. A molecular docking study was implemented with the acetylcholinesterase of the electric eel (*Electrophorus electricus*) (EeAChE) and with the horse (*Equus caballus*) butyrylcholinesterase (EcBChE) in order to get insight of possible reasons for the observed enzyme inhibition data at the molecular level. Cholinesterases have two known binding sites: the active site, where the enzymes hydrolyse their substrates; and the peripheral site, both located at the extremities of a gorge in the enzyme structure.³¹ Both sites were explored in the docking study, to determine which one is the most suitable for the binding of these compounds.

We implemented redocking experiments as a previous test for the ability of the docking program GOLD 5.6 (CCDC Software Ltd., Cambridge, UK) to find reliable solutions for the docking to cholinesterases. Since all EeAChE structures accessible in the Protein Data Bank (PDB) do not have ligands in their crystallographic structures, the scoring functions available in the program were tested through redocking procedures with the PDB structure 2CMF (Torpedo californica AChE co-crystallized with alkylene-linked bis-tacrine dimer).²⁴ Hydrogen atoms were added to proteins structures based on ionization and tautomeric states defined by GOLD. The bonds of groups capable to donate hydrogen bonds present in serine, threonine, tyrosine and lysine side chains were set free to rotate during the docking procedure to allow the best orientation of the hydrogen bonds. In the course of the searching procedure, 100 000 genetic operations (crossover, migration, mutation) were used for each docking run. Radius of binding sites for the enzymes was tested at 15 \AA and 20 \AA around atoms from adequate amino acids selected based on literature information for each binding site. The same score function, corresponding amino acids and radius were adopted for the docking studies with the EcBChE model.

Three EeAChE structures are available in PDB, with codes 1EEA,³² 1C2B³³ and 1C2O³⁴ and all of them were evaluated in our docking studies. There is no available crystallographic structure for EcBChE, so it was necessary the construction of a 3D model from a sequence available in the UniProtKB/Swiss-Prot protein sequence database (entry Q9N1N9) with the protein structure homology-modelling server, Swiss-Model,³¹ as previously described,²⁴ using as a template the human BChE with PDB code 4TPK.³⁵ The resolution of the template is 2.52 \AA , the identity between sequences is 90.40%, with a coverage 0.95. The global and per-residue model quality has been assessed using the QMEAN scoring function.

In the GOLD program, the docking functions yield the "fitness scores", which are dimensionless values. The score of each pose identified is calculated as the negative of the sum of a series of energy terms involved in the protein-ligand interaction process, so that the more positive the score, the better is the interaction. The score values are a guide of how good the



docking pose is, with a higher score indicating a better interaction between the ligand and the binding site.

Spartan'14 program [Wavefunction, Inc.] was utilized to construct and optimize the molecules in study, with the PM6 method. Since these compounds have two plausible protonation sites in the piperazine ring, structures protonated at each of them and also with both of them protonated were considered in our studies. Several poses were obtained for each compound in all proteins, and the best-ranked pose for each one was chosen for analysis of the interactions with the amino acid residues.

Conflicts of interest

There is no conflict to declare.

Acknowledgements

Fellowship and financial support for this study was provided by Conselho Nacional de Desenvolvimento Científico e Tecnológico - Brasil (CNPq), Fundação de Amparo à Pesquisa do Estado do Rio de Janeiro - Brasil (FAPERJ) and Coordenação de Aperfeiçoamento de Pessoal de Nível Superior - Brasil (CAPES) - Finance Code 001.

Notes and references

- 1 S. Borg, G. Estenne-Bouhtou, K. Luthman, I. Csöreg, W. Hesselink and U. Hacksell, *J. Org. Chem.*, 1995, **60**, 3112.
- 2 E. Bozo, G. Szilagyí and J. Janaky, *Arch. Pharm.*, 1989, **322**, 583.
- 3 Y. Naito, F. Akahoshi, S. Takeda, T. Okada, M. Kajii, H. Nishimura, M. Sugiura, C. Fukaya and Y. J. Kagitani, *J. Med. Chem.*, 1996, **39**, 3019.
- 4 J. P. Marino, P. W. Fisher, G. A. Hofmann, R. B. Kirkpatrick, C. A. Janson, R. K. Johnson, C. Ma, M. Mattern, T. D. Meek, M. D. Ryan, C. Schulz, W. W. Smith, D. G. Tew, T. A. Tomazek, D. F. Veber, W. C. Xiong, Y. Yamamoto, K. Yamashita, G. Yang and S. K. Thompson, *J. Med. Chem.*, 2007, **50**, 3777.
- 5 J.-L. Fauchere, J.-C. Ortuno, J. Duhault, J. A. Boutin and N. Levens, European Patent EP 1044970, 2000.
- 6 G. Winterer, J. Gallinat, J. Brinkmeyer, F. Musso, J. Kornhuber, N. Thuerauf, D. Rujescu, R. Favis, Y. Sun, M. A. Franc, S. Ouwerkerk-Mahadevan, L. Janssens, M. Timmers and J. R. Streffer, *Neuropharmacology*, 2013, **64**, 197.
- 7 (a) S. Maddila, R. Pagadala and S. B. Jonnalagadda, *Lett. Org. Chem.*, 2013, **10**, 693; (b) J. Meng and P. P. Kung, *Tetrahedron Lett.*, 2009, **50**, 1667; (c) G. M. Makara, Y. Ma and L. Margarida, *Org. Lett.*, 2002, **4**, 1751; (d) A. V. Bogolyubsky, O. Savych, A. V. Zhemera, S. E. Pipko, A. V. Grishchenko, A. I. Konovets, R. O. Doroshchuk, D. N. Khomenko, V. S. Brovarets, Y. S. Moroz and M. Vybornyi, *ACS Comb. Sci.*, 2018, **20**, 461.
- 8 A. R. Katritzky, B. V. Rogovoy, V. Y. Vvedensky, K. Kovalenko, P. J. Steel, V. I. Markov and B. Forood, *Synthesis*, 2001, **6**, 897.
- 9 Y. Yu, J. M. Ostresh and R. A. Houghten, *Tetrahedron Lett.*, 2003, **44**, 7841.
- 10 D. G. Churchill, *J. Chem. Educ.*, 2006, **83**, 1798.
- 11 A. A. Schiltand, L. C. McBride, *Perchloric Acid and Perchlorates*, ed. G. F. Smith, Chemical Co, Columbus (USA), 2003.
- 12 J. Shen, B. Wong, C. Gu and H. Zhang, *Org. Lett.*, 2015, **17**, 4678.
- 13 (a) D. Garella, E. Borretto, A. Di Stilo, K. Martina, G. Cravotto and P. Cintas, *Med. Chem. Commun.*, 2013, **4**, 1323; (b) N. M. Nascimento-Júnior, A. E. Kümmerle, E. J. Barreiro and C. A. M. Fraga, *Molecules*, 2011, **16**, 9274.
- 14 S. M. Hickey, T. D. Ashton, S. K. Khosa, R. N. Robson, J. M. White, J. Li, R. L. Nation, H. Y. Yu, A. G. Elliott, M. S. Butler, J. X. Huang, M. A. Cooperd and F. M. Pfeffer, *Org. Biomol. Chem.*, 2015, **13**, 6225.
- 15 R. Anand, K. D. Gill and A. A. Mahdi, *Neuropharmacology*, 2014, **76**, 27.
- 16 A. V. Terry and J. J. Buccafusco, *J. Pharmacol. Exp. Ther.*, 2003, **306**, 821.
- 17 C. P. Ferri, M. Prince, C. Brayne, M. Ganguli, K. Hall, K. Hasegawa, H. Hendrie, Y. Huang, A. Jorm, C. Mathers, P. R. Menezes, E. Rimmer and M. Sczufca, *Lancet*, 2005, **366**, 2112.
- 18 A. Sinha, R. S. Tamboli, B. Seth, A. M. Kanhed, S. Kant Tiwari, S. Agarwal, S. Nair, R. Giridhar, R. K. Chaturvedi and M. R. Yadav, *Mol. Neurobiol.*, 2015, **52**, 638.
- 19 L. M. Lima and E. J. Barreiro, *Curr. Med. Chem.*, 2005, **12**, 23.
- 20 C. Viegas-Junior, A. Danuello, V. d. S. Bolzani, E. J. Barreiro and C. A. Fraga, *Curr. Med. Chem.*, 2007, **14**, 1829.
- 21 G. L. Ellman, K. D. Courtney, V. Andres and R. M. Featherstone, *Biochem. Pharmacol.*, 1961, **7**, 88.
- 22 H. Sugimoto, Y. Iimura, Y. Yamanishi and K. Yamatsu, *J. Med. Chem.*, 1995, **24**, 4821.
- 23 G. Jones, P. Willett, R. C. Glen, A. R. Leach and R. Taylor, *J. Mol. Biol.*, 1997, **267**, 727.
- 24 E. H. Rydberg, B. Brumshtein, H. M. Greenblatt, D. M. Wong, D. Shaya, L. D. Williams, P. R. Carlier, Y. P. Pang, I. Silman and J. L. Sussman, *J. Med. Chem.*, 2006, **49**, 5491.
- 25 G. A. de Souza, S. J. da Silva, C. N. Del Cistia, P. Pitas-Santos, L. O. Pires, Y. M. Passos, Y. Cordeiro, C. M. Cardoso, R. N. Castro, C. M. R. Sant'Anna and A. E. Kümmerle, *J. Enzyme Inhib. Med. Chem.*, 2019, **34**, 631.
- 26 D. Antoine, M. Olivier and Z. Vincent, *Sci. Rep.*, 2017, **7**, 42717.
- 27 D. Antoine and Z. Vincent, *ChemMedChem*, 2016, **11**, 1117.
- 28 C. A. Lipinski, F. Lombardo, B. W. Dominy and P. J. Feeney, *Adv. Drug Delivery Rev.*, 2001, **46**, 3.
- 29 D. F. Veber, R. J. Stephen, C. Hung-Yuan, B. R. Smith, K. W. Ward and K. D. Kopple, *J. Med. Chem.*, 2002, **45**, 2615.
- 30 W. J. Egan, K. M. Merz and J. J. Baldwin, *J. Med. Chem.*, 2000, **43**, 3867.
- 31 L. Pezzementi, F. Nachon and A. Chatonnet, *PLoS One*, 2011, **6**, e17396.
- 32 M. L. Raves, K. Giles, J. D. Schrag, M. F. Schmid, G. N. Phillips Jr, W. Chiu, A. J. Howard, I. Silman and J. L. Sussman, Quaternary Structure of Tetrameric



- Acetylcholinesterase, in *Structure and Function of Cholinesterases and Related Proteins*, ed. B. P. Doctor, P. Taylor, D. M. Quinn, R. L. Rotundo and M. K. Gentry, Springer, Boston, MA, 1998.
- 33 Y. Bourne, J. Grassi, P. E. Bougis and P. Marchot, *J. Biol. Chem.*, 1999, **274**, 30370.
- 34 M. Biasini, S. Bienert, A. Waterhouse, K. Arnold, G. Studer, T. Schmidt, F. Kiefer, T. G. Cassarino, M. Bertoni, L. Bordoli and T. Schwede, *Nucleic Acids Res.*, 2014, **42**, W252.
- 35 B. Brus, U. Kosak, S. Turk, A. Pisljar, N. Coquelle, J. Kos, J. Stojan, J. P. Colletier and S. Gobec, *J. Med. Chem.*, 2014, **57**, 8167.

